Contents lists available at ScienceDirect

Food Bioscience

journal homepage: http://ees.elsevier.com

Metabolite profiling of three *Opuntia ficus-indica* fruit cultivars using UPLC-QTOF-MS in relation to their antioxidant potential

Mohamed A. Farag [a,b,*], Ibrahim E. Sallam [c], Mostafa I. Fekry [a], Soumaya S. Zaghloul [c], Riham S. El-Dine [a]

[a] Pharmacognosy Department, College of Pharmacy, Cairo University, Cairo, 11562, Egypt
[b] Department of Chemistry, School of Sciences & Engineering, The American University in Cairo, New Cairo, 11835, Egypt
[c] Pharmacognosy Department, College of Pharmacy, October University for Modern Sciences and Arts (MSA), 6th of October City, 12566, Egypt

ARTICLE INFO

Keywords
Opuntia ficus-Indica
Isorhamnetin
Coumarin
Chemometrics
Dihydroxy psoralen-*O*-Hexoside

ABSTRACT

Opuntia ficus-indica is the economically important cactus species belonging to the Cactaceae family. Its importance arises from its nutritional value and various biological activities such as antioxidant, anticancer and antimicrobial activities. This study attempts to characterize the metabolic profile of three *O. ficus* cultivars having different colors, *i.e.,* red 'Rose', greenish white 'Bianca' and yellow-orange represented by peels and pulp tissues using ultra-performance liquid chromatography coupled to high resolution time of flight mass spectrometry (UPLC-QTOF-MS). A total of 45 metabolites were identified mainly flavonoids: isorhamnetin conjugates and phenolic acids, whereas betaxanthins and coumarins were present at lower levels. Principle component analysis and orthogonal projection discriminant analysis showed that dihydroxy psoralen-*O*-hexoside and glycosidic conjugates of ferulic acid were the most discriminatory metabolites among the peels and pulps within the different cultivars. On the other hand, the level of flavonoids was comparable among the cultivars. The antioxidant activity of peels and pulps extracts were further measured using 2,2-diphenyl-1-picrylhydrazyl and 2,2′-azino-bis(3-ethylbenzothiazoline-6-sulphonic acid) assays. ''Rose'' cultivar peel rich in dihydroxy psoralen-*O*-hexoside showed the highest antioxidant activity in both assays. This suggested that coumarins and flavonoids mediated high antioxidant activity of *O. ficus-indica* fruits although present at low levels.

1. Introduction

Opuntia ficus-indica is a widespread and commercially important cactus fruit belonging to family Cactaceae (Fernie, Trethewey, Krotzky, & Willmitzer, 2004). It is indigenous to Mexico and widely distributed in other regions such as Africa, Australia, and the Mediterranean region including Egypt (Mata et al., 2016). The *Opuntia* genus encompasses 1500 species highly valued for their nutritional composition and/or biological activities (Ammar, Ennouri, Bouaziz, Ben Amira, & Attia, 2015). Bioactive secondary metabolites reported in *O. ficus* include phenolic acids, flavonoids and betalains. Betalains are water-soluble nitrogen containing pigments that are classified into betacyanins or betaxanthins (Fig. 1), conjugates of betalamic acid. Betalains are used mainly as natural food colorants (Melgar et al., 2017). Moreover, the antioxidant property of *O. ficus* makes it a potential prophylactic for many degenerative diseases (Ginestra et al., 2009). The antioxidant activity of *O. ficus* fruit is reported to be twice as high as that of pears, apples, tomatoes and bananas, while it is comparable to red grapes and grapefruit (Albano et al., 2015). In a previous study, the aroma and metabolites of the three cultivars (cvs) were investigated using UV–vis fingerprinting and gas chromatography coupled to mass spectroscopy. Betalains were abundant in the red cv, while carotenoids and chlorophyll were more abundant in the green and orange cvs. Previously the primary metabolites mediating the cvs taste and nutritional values were profiled using GC-MS post-silylation with 82 metabolites identified, and with glucose and fructose accounting for the most abundant sugars, while proline as the major free amino acid (Farag, Maamoun, Ehrlich, Fahmy, & Wesjohann, 2017) (see Fig. 2).

Likewise, the same *O. ficus* species can show different phytochemical compositions when grown in various regions. There is little data about the chemical composition of the different cvs of *O. ficus* fruit. Therefore, the aim of this study was to assess metabolite heterogeneity within peel and pulp tissues of *O. ficus* fruit cvs having different colors; red 'Rose', greenish white 'Bianca' and yellow-orange 'Gialla' (Table 1) in relation to their antioxidant properties as analyzed using multivariate data analyses.

To provide a broad coverage of the *O. ficus*-indica secondary metabolome in an untargeted manner and pinpoint differential secondary metabolite accumulation among these cvs, metabolite profiling was used. Metabolites profiling and/or fingerprinting aims to create a broad image of the system studied at a quantitative level (Wolfender, Marti, Thomas, & Bertrand, 2015). The ficus fruit secondary metabolome was assessed using advanced hyphenated chromato-

* Corresponding author. Pharmacognosy Department, College of Pharmacy, Cairo University, Cairo, 11562, Egypt.
E-mail address: mfarag73@yahoo.com (M.A. Farag)

https://doi.org/10.1016/j.fbio.2020.100673
Received 28 March 2019; Received in revised form 2 June 2020; Accepted 2 June 2020
Available online xxx

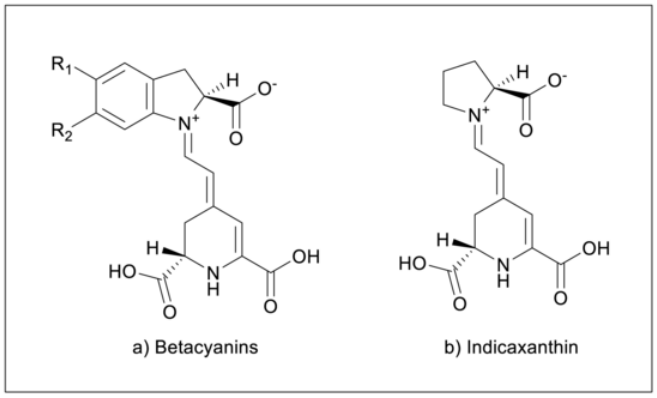

Fig. 1. Chemical structures of the most common betalains found in *O. ficus* cvs; a) betacyanins; betanidin (R_1 and R_2 = H), betanin (R_1 = glucose, R_2 = H) and b) indicaxanthin.

graphic techniques of coupled ultra-performance liquid chromatography to high resolution time of flight mass spectrometer (UPLC-QTOF-MS). This platform was adopted due to the complex nature of plant extracts with numerous classes of secondary metabolites, which would be difficult to analyze using classical analytical techniques such as HPLC. Due to the high resolution of UPLC peaks, in addition to the high accuracy and sensitivity of QTOF-MS, many metabolites can be detected within a crude plant extract (Fernie et al., 2004; Seger & Sturm, 2007). Additionally, multivariate data analyses such as principle component analysis (PCA) and orthogonal projection discriminant analysis (OPLS-DA) were used. Such bioinformatic tools have been increasingly used for the geographic and chemotaxonomic classification of food and plant products (Farag et al., 2017; Seger & Sturm, 2007). The antioxidant activity of crude extracts was monitored spectrophotometrically using two assays: free radical scavenging activity; *i.e.*, the 2,2-diphenyl-1-picrylhydrazyl (DPPH) and cation radical scavenging activity; *i.e.*, 2,2′-azino-bis(3-ethylbenzothiazoline-6-sulphonic acid) (ABTS) assays. The data from these antioxidant assays along with the information derived from the metabolite profiling could help in determining which cv ought to be selected for further agricultural development to be used as a functional food.

2. Material and methods

2.1. Plant material and chemicals

Fresh samples from three cvs of *O. ficus*; red 'Rose', yellow-orange 'Gialla' and greenish-white 'Bianca' fruits were purchased from L′ Organizzazione Produttori (O.P.) Eurocitrus, SRL (Sicily, Italy) in July 2015. Fruits were harvested when fully mature ranging in size from 4 to 9 cm (length) and 3–5 cm (diameter). Fruits were peeled using a razor blade. Fruits were lyophilized as whole parts using a Stellar® Laboratory Freeze Dryer, (Millrock, Inc., New York, NY, USA), stored at −20 °C, and extracted within 1–2 wk for metabolite analysis. Voucher specimens of freeze-dried fruits were placed in the Pharmacognosy Department, Faculty of Pharmacy, Cairo University (Cairo, Egypt). Standards for isorhamnetin, isorhamnetin glucoside and quercetin glucoside were purchased from Sigma Aldrich Co. (St. Louis, MO, USA).

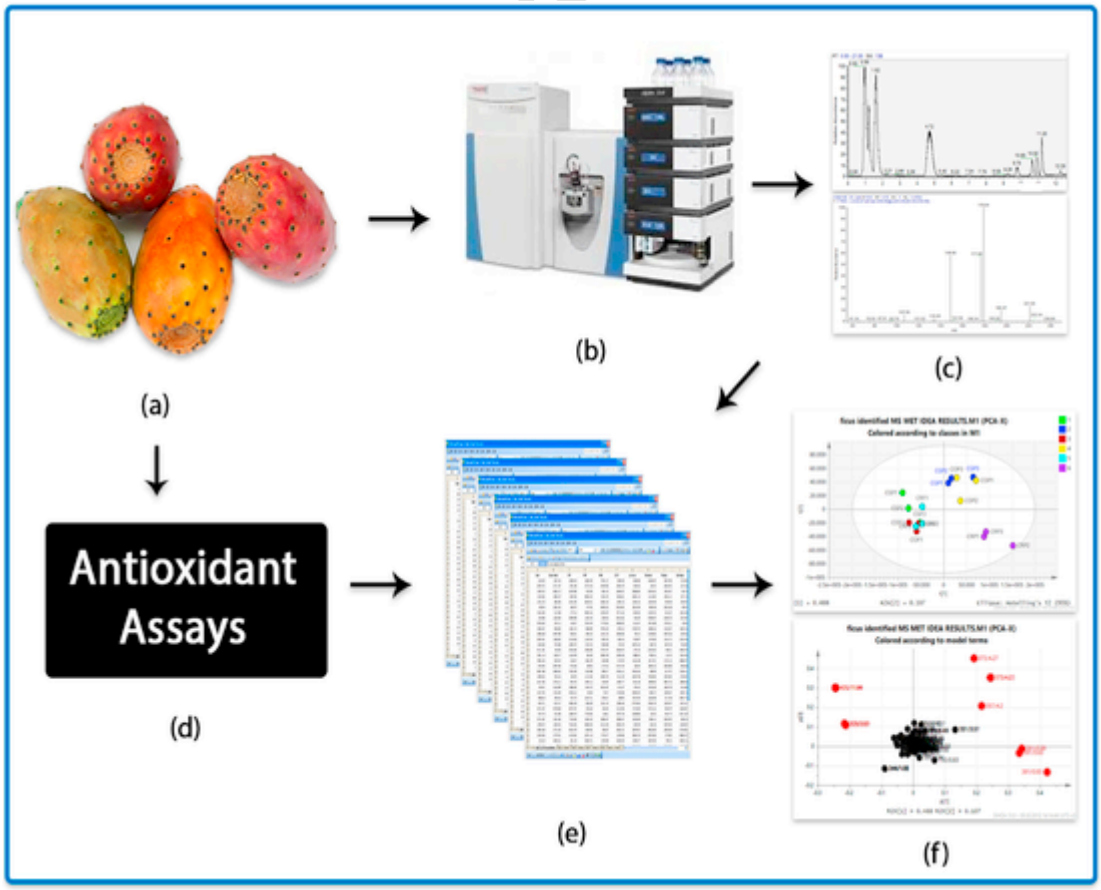

Fig. 2. Experimental workflow showing steps done in exact order; a) methanol extraction of the peels and pulps of three cvs of *Opuntia ficus-indica* fruits, b) identification of phytoconstituents of the methanol extracts using reversed-phase UPLC/PDA/ESI-qTOF-MS, c) metabolites identification, d) determination of the antioxidant activities of the methanol extracts using DPPH and ABTS assays, e) MS abundance data extraction, f) multivariate data analysis of UPLC/MS dataset using unsupervised principle component analysis and supervised orthogonal projection to latent structures-discrimination with score and loading plots.

Table 1
Name and sample codes of *O.ficus-indica* cvs peels and pulps.

Sample code	Cultivar name
CGF	Greenish white 'Bianca' cv pulp
CGP	Greenish white 'Bianca' cv peel
COF	Yellow-orange 'Gialla' cv pulp
COP	Yellow-orange 'Gialla' cv peel
CRF	Red 'Rose' cv pulp
CRP	Red 'Rose' cv peel

2.2. Extraction procedure and sample preparation of pulps and peels

The dried peel and pulp of each cv (150 mg) was homogenized with methanol (6 ml) containing 5 μg ml^{-1} umbelliferone as an internal standard, (Sigma Aldrich) using a T 18 digital Ultra-Turrax mixer (IKA Dispersers, Staufen, Germany) set at 11,000 rpm for 20 s for 5 periods. Each mixing period was separated by 1 min to prevent heating. To remove plant debris, extracts were vortexed using a Vortex mixer (VWR®, Radnor, PA, USA) then centrifuged at 3,000*g* (Thermo Fisher Scientific, Waltham, MA, USA) for 30 min. For further purification, 500 μl of the methanol extracts were placed on a 500 mg Sep-Pak C18 3 cc, 55–105 μm C18 cartridge 3 × 0.25 cm (Agilent Technologies, Santa Clara, CA, USA) preconditioned with 2 ml methanol followed by 2 ml water. Samples were eluted using 3 ml 100% methanol. The eluent was evaporated to dryness under a stream of nitrogen at room temperature (28 °C). The residue was re-suspended in 300 μl methanol and 3 μl was injected for UPLC-MS analysis using chromatographic conditions that have been successfully used for profiling similar plant matrices (De Leo, Abreu, Pawlowska, Cioni, & Braca, 2010; Guevara-Figueroa et al., 2010; Mata et al., 2016).

2.3. High-resolution UPLC-PDA-MS analysis

Chromatographic separation was done on an Acuity UPLC system (Waters Corp., Milford, MA, USA) equipped with a HSS T3 column (100 × 1.0 mm, particle size 1.8 μm; Waters). The analysis was carried out by applying the following binary gradient at a flow rate of 150 μl min^{-1}: 0–1 min, isocratic 95% A (water containing 0.1% formic acid), 5% B (acetonitrile containing 0.1% formic acid); 1–16 min, gradient from 5 to 95% B; 16–18 min, isocratic 95% B; 18–20 min, isocratic 5% B. The injection volume was 3.1 μl (full loop injection). Eluted compounds were detected with UV–vis and MS. Scan range of the UV was 200–600 nm, and, MS was 100–1000 *m/z* for the negative ion mode and 220–1000 *m/z* for the positive ion mode using the following instrument settings: nebulizer gas, nitrogen, 1.6 bar; dry gas, nitrogen, 6l min^{-1}, 190 °C; capillary, -5.5 kV; in-source collision-induced dissociation (CID) energy, 0 V; hexapole radio frequency (RF), 100 Vpp; quadrupole ion energy, 5 eV; collision gas, argon; collision energy, 10 eV; collision RF 200/400 Vpp (timing 50/50); transfer time, 70 μs; prepulse storage, 5 μs; pulser frequency, 10 kHz; spectra rate, 3 Hz. Internal mass calibration of each analysis was done by infusing 20 μl 10 mM lithium formate in isopropanol:water, 1:1 (v/v), at a gradient time of 18 min using a diverter valve.

2.4. Identification and quantification of metabolites and MS data multivariate analysis

Metabolite identification used the UV–vis spectra (220–600 nm), retention time relative to external standards, mass spectra, and comparison with reference literature. Furthermore, tandem mass data was used to confirm the identity of the compound. Relative quantification of metabolites, detected with MS, was done using XCMS™ data analysis software (The Scripps Research Institute, La Jolla, CA, USA). PCA on the MS data was done using a custom script within the R 2.9.2 environment. OPLS-DA was done with SIMCA-P Version 13.0 (Umetrics, Umeå, Sweden).

2.5. Extraction procedure and sample preparation for antioxidant assay

The freeze-dried pulps and peels were homogenized using a FusionBlade blender (Black and Decker Corp., Beachwood, OH, USA) at speed setting of 6 for 10 min. Extracts were obtained using cold maceration of fruit materials in 100% MeOH with shaking for 5 h at ~28 °C until exhaustion, *i.e.*, no color is observed within the extract followed by filtration using wet cotton. The residue was further extracted twice for 15 min each. Methanol extracts were combined, concentrated in a vacuum, and subsequently freeze-dried and stored at −20 °C for 3 months during which the analyses were done. The dry residue (10 mg) was dissolved in methanol to obtain the following concentrations 100, 10, 5, and 2.5 μg ml^{-1} to calculate IC_{50} using the following antioxidants assays. IC_{50} were derived from three independent biological replicates of fruit extracts prepared using the same conditions.

2.6. DPPH assay

The antioxidant capacity was determined by scavenging the DPPH radical as described in Farag, Handoussa, Fekry, and Wessjohann (2016). Methanol extract (50 μl) was mixed with 2 ml 0.09 mM DPPH solution using a shaker at 25 °C and 1000 rpm followed by incubation at room temperature for 15 min in the dark. Absorbance was measured at 517 nm using a Beckman Coulter DTX 880 microplate reader (Biodirect Corp., Taunton, MA, USA). Ascorbic acid was used as a positive control. Blank samples were prepared by replacing the methanol extract with pure methanol. Triplicates were done for each measurement prepared from different specimen using the same conditions.

2.7. ABTS assay

The total antioxidant activity of the samples was measured using an ABTS radical cation decolorization assay according to the method described by Albano et al. (2015). ABTS was produced by reacting 7 mM ABTS aqueous solution with 2.4 mM potassium persulfate in the dark for 12–16 h at room temperature. Two ml of diluted ABTS solution was added to 20 μl (1 mg ml^{-1}) sample. After 30 min of incubation at room temperature, the absorbance was measured at 734 nm using the microplate reader. Ascorbic acid was used as a reference standard. Triplicates were done for each measurement prepared from different specimen under the same conditions.

2.8. Statistical analysis

Statistical analysis was carried out using one-way analysis of variance (ANOVA) with Graph Pad Prism version 6 (GraphPad, San Diego, CA, USA). The significant difference between the means was compared using the honest significant difference (HSD) as obtained using Tukey's post hoc test at the $p < 0.05$ level. All results were expressed as mean ± standard error of the mean.

3. Results and discussion

3.1. Metabolite identification using UPLC-MS analysis

The secondary metabolites of peels and pulps of the three fruit cvs were determined using UPLC-QTOF-MS. Two major metabolite classes were identified; phenolic acids and flavonoids, in addition to other minor classes, *i.e.*, coumarins and betalains. The chromatographic separation led to the detection of 27 and 49 metabolite peaks in negative and positive modes, respectively, were observed (Table 2). A complete

Table 2
Metabolites identified in *O. ficus-indica* methanol extract using UPLC/PDA/ESI-qTOF-MS in both negative and positive ionization modes.

Peak no.	[M-H]$^-$	[M+H]$^+$	Rt $_{(sec)}$	UV	Molecular formula	Error $_{(ppm)}$	MS/MS	Identification	Class
1	109.04	-	9	nd	-	-	-	-	-
2	106.04	-	10	nd	$C_7H_6O^-$	-0.72	79.03, 65.02	-	-
3	195.05	-	58	nd	$C_6H_{11}O_7^-$	5.23	177.04, 159.03, 129.02	Gluconic acid	Organic acid
4	-	381.07	58	272, 369	$C_{17}H_{17}O_{10}^+$	-1.9	219.03, 203.03, 187.07, 131.61	Dihydroxy psoralen-*O*-hexoside	Coumarin
5	191.02	-	59	273, 479	$C_6H_7O_7^-$	7.75	111.01	(Iso)Citric acid	Organic acid
6	-	309.1	95	269, 479	$C_{14}H_{17}O_6N_2^+$	-0.46	265.12, 263.10, 219.11	Indicaxanthin	Betalain
7	255.05	-	97	223, 276	$C_{11}H_{11}O_7^-$	5.68	237.04, 193.05, 165.06	Piscidic acid	Phenolic acid
8	-	322.21	110	nd	$C_{17}H_{28}O_3N_3^+$	0.005	305.19, 265.15, 248.13, 177.05	-	-
9	-	265.11	115	nd	$C_{13}H_{17}O_4N_2^+$	-0.57	221.13, 178.09	-	-
10	-	367.14	141	nd	$C_{17}H_{23}O_7N_2^+$	-0.45	349.14, 229.10	-	-
11	179.05	-	256	nd	$C_6H_{11}O_6^-$	7.45	161.01, 135.05	Hexose	Sugar
13	-	217.04	271	nd	-	1.9	206.13	-	-
14	-	344.13	271	nd	$C_{12}H_{24}O_{11}^+$	7.8	309.10, 165.05, 147.04	*p*-Coumaric acid derivative	Phenolic acid
15	-	223.06	281	nd	$C_{11}H_{11}O_5^+$	1.61	205.05, 195.07, 177.05	Ferulic acid derivative	Phenolic acid
16	239.05	-	283	223, 276	$C_{11}H_{11}O_6^-$	4.87	179.04, 149.06	Eucomic acid	Phenolic acid
17	349.18	-	383	nd	$C_{17}H_{31}O_{10}^-$	2.21	349.19	p-Menthane-triol hexoside	-
18	-	379.09	407	nd	$C_{18}H_{19}O_9^+$	-6.35	217.05, 185.04	β-Sorigenin hexoside	-
19	355.1	-	422	328, 369	$C_{16}H_{19}O_9^-$	3.44	193.05, 175.04, 134.04	Ferulic acid hexoside	Phenolic acid
20	959.32	-	455	nd	$C_{57}H_{51}O_{14}^-$	-5.4	783	Unknown glycoside	-
21	371.09	-	458	nd	$C_{16}H_{19}O_{10}^-$	0.88	249.06, 193.04, 175.02	Feruloyl gluconic acid	Phenolic acid
22	-	325.13	541	nd	$C_{12}H_{21}O_{10}^+$	0.05	307.13, 191.08	Unknown disaccharide	Sugar
23	391.23	-	547	nd	$C_{19}H_{35}O_8^-$	1.85	276.35	Megastigmane triol hexoside	-
24	489.16	491.17	550/560	327	$C_{21}H_{29}O_{13}^-$/$C_{21}H_{31}O_{13}^+$	1.39/-0.34	235.06, 193.05, 175.04	Caffeoyl glycoside	Phenolic acid
25	-	339.1	569	327	$C_{16}H_{19}O_8^+$	-1.04	321.10, 195.07, 177.05	*p*-Coumaroylquinic acid	Phenolic acid
26	-	898.3	575	370	$C_{37}H_{54}O_{25}^+$	3.93	752.24, 637.18, 491.12, 329.07, 314.04	Unknown flavonoid	Flavonoid
27	537.19	-	575	nd	$C_{26}H_{33}O_{12}^-$	0.57	375.14, 195.07	Unknown glycoside	-
28	-	884.28	580	nd	$C_{36}H_{52}O_{25}^+$	2.43	637.18, 491.12, 329.07, 314.04	Unknown flavonoid	Flavonoid
29 [a]	-	465.18	595	nd	$C_{21}H_{21}O_{12}^+$	-22.1	447.18, 303.05	Quercetin-*O*-hexoside	Flavonoid
30	-	470.22	599	nd	$C_{22}H_{34}O_9N_2^+$	1.74	309.20, 219.11	-	-
31	741.18	-	607	nd	$C_{32}H_{38}O_{20}^-$	-0.67	609.15, 301.3	Quercetin-*O*-pentosyl-rutinoside	Flavonoid
32	-	757.21	613	nd	$C_{33}H_{41}O_{20}^+$	-1.86	465.10, 303.05	Quercetin-*O*-dirhamnosyl hexoside	Flavonoid
33	-	352.15	616	nd	$C_{14}H_{26}O_9N^+$	-0.93	249.06, 231.05	-	-
34	785.21	787.22	619/626	nd	$C_{34}H_{41}O_{21}^-$/$C_{34}H_{43}O_{21}^+$	-0.71/-3.02	639.16, 477.10, 315.05	Isorhamnetin-*O*-di-hexosyl-rhamnoside	Flavonoid
35	613.21	-	622	nd	$C_{28}H_{37}O_{15}^-$	-0.17	405.15, 357.13, 195.07	-	-
36	611.25	-	625	nd	$C_{26}H_{43}O_{16}^-$	0.42	431.19, 251.13	-	-
37	387.2	-	629	nd	$C_{19}H_{31}O_8^-$	1.69	225.15, 179.05, 161.05	Caffeic acid derivative	Phenolic acid
38	-	484.24	634	nd	$C_{23}H_{36}O_9N_2^+$	5.75	309.20, 219.11	-	-
39	769.21	771.23	634/635	254, 355	$C_{34}H_{41}O_{20}^-$/$C_{34}H_{43}O_{20}^+$	-0.31/-0.59	605.15, 477.61, 315.05	Isorhamnetin-*O*-hexosyl-di-rhamnoside	Flavonoid
40	755.2	757.21	639/637	254, 355	$C_{33}H_{39}O_{20}^-$/$C_{33}H_{41}O_{20}^+$	1.48/-1.21	623.16, 605.15, 315.05	Isorhamnetin-*O*-pentosyl-rutinoside	Flavonoid
41	565.19	-	651	nd	$C_{27}H_{33}O_{13}^-$	1.01	339.12, 327.12	-	-
42	609.14	611.16	655/659	254, 355	$C_{27}H_{29}O_{16}^-$/$C_{27}H_{31}O_{16}^+$	1.31/0.57	459.09, 315.05	Isorhamnetin-*O*-pentosyl-hexoside	Flavonoid
43	623.16	625.17	672/675	251, 350	$C_{28}H_{31}O_{16}^-$/$C_{28}H_{33}O_{16}^+$	1.6 [a]/0.12	315.05	Isorhamnetin-*O*-rutinoside	Flavonoid

Table 2 (*Continued*)

Peak no.	[M-H]$^-$	[M+H]$^+$	Rt $_{(sec)}$	UV	Molecular formula	Error $_{(ppm)}$	MS/MS	Identification	Class
44 [a]	477.1	-	684	nd	$C_{22}H_{21}O_{12}^-$	0.97	315.05	Isorhamnetin-*O*-hexoside	Flavonoid
45	-	498.26	691	nd	$C_{13}H_{38}O_{12}N_8^+$	-0.3	322.21, 234.11	-	-
46	-	693.27	699	nd	$C_{34}H_{45}O_{15}^+$	1.54	675.26, 319.13	Isorhamnetin-*O*-glycoside	Flavonoid
47	371.2	-	706	nd	$C_{19}H_{31}O_7^-$	0.63	209.12, 181.05, 166.03	Hydroxy-megastigmen-one-hexoside	Terpene
48	-	665.28	715	nd	$C_{33}H_{45}O_{15}^+$	0.11	647.27, 303.13	-	Flavonoid
49	-	480.28	727	nd	$C_{22}H_{23}O_{12}^+$	0.57	445.24, 317.07	Isorhamnetin-*O*-glycoside	Flavonoid
50	-	679.29	733	nd	$C_{35}H_{43}O_{10}N_4^+$	0.17	647.27, 522.22, 464.22	-	-
51	-	459.22	733	nd	$C_{22}H_{35}O_{10}^+$	-0.49	441.21, 211.17	Hydroxy-megastigmen derivative	Terpene
52	431.09	-	737	221, 329	$C_{21}H_{19}O_{10}^-$	2.93	237.04, 193.05, 165.06	Feruloyl piscidic acid	Phenolic acid
53	-	817.21	738	nd	$C_{38}H_{41}O_{20}^+$	-1.79	685.18, 553.43, 479.12, 317.07	Unknown flavonoid glycoside	Flavonoid
54	-	289.07	750	nd	$C_{15}H_{13}O_6^+$	1.09	271 [a]06, 179.03, 163.04, 145.03, 135.04	Eriodictyol	Flavonoid
55	-	241.2	764	nd	$C_{14}H_{27}O_2N^+$	1.32	123.12	-	-
56 [a]	-	317.06	822	nd	$C_{16}H_{13}O_7^+$	0.003	303.05, 285.04, 177.05	Isorhamnetin	Flavonoid
57	-	307.26	828	nd	$C_{20}H_{35}O_2^+$	0.79	289.25, 271.24, 179.14, 163.15, 135.12	Unknown diterpene	Terpene
58	-	323.25	829	nd	$C_{18}H_{33}O_2N_3^+$	1.64	305.25, 151.15	-	-
59	-	301.07	831	nd	$C_{16}H_{31}O_6^+$	-0.54	286.05	Dihydroxyhexadecanoic acid	Fatty acid
60	-	293.28	871	nd	$C_{20}H_{37}O^+$	0.46	275.27	-	-
61	-	279.09	901	nd	$C_{16}H_{22}O_4^+$	0.48	201.05, 149.02	-	-
62	-	271.18	909	nd	$C_{15}H_{11}O_5^+$	1.06	229.86, 215.10	Trihydroxyflavone	Flavonoid
63	-	228.1	915	nd	$C_3H_{14}O_5N_7^+$	-0.4	172.04	-	-
64	-	313.1	918	nd	$C_{18}H_{17}O_5^+$	-1.15	298.08, 252.05	Trimethoxyflavone	Flavonoid
65	-	255.15	923	nd	$C_{14}H_{23}O_4^+$	1.6	237.17, 195.14, 176.00	-	-
66	-	226.12	936	nd	$C_{15}H_{16}ON^+$	1.54	181.10, 148.08, 91.05	-	-
67	-	277.17	946	nd	$C_{14}H_{29}O_5^+$	1.84	235.17	-	-
68	-	311.18	954	nd	$C_{17}H_{27}O_5^+$	-0.29	293.17, 255.12, 237.11	-	-
69	-	256.04	980	nd	$C_{11}H_6O_3N_5^+$	-0.13	199.98, 181.97	-	-
70	-	261.18	986	nd	$C_{17}H_{25}O_2^+$	0.35	219.17, 205.12	-	-
71	-	299.18	988	nd	$C_{18}H_{27}O_5^+$	0.41	212.05	-	-
72	-	353.26	1002	nd	$C_{21}H_{37}O_4^+$	0.46	261.22, 243.21	Unknown steroid	Steroid
73	-	476.27	1012	nd	$C_{27}H_{40}O_7^+$	1.29	335.26	-	-
74	-	318.29	1033	nd	$C_{18}H_{40}O\ ^aN^+$	-0.88	300.29, 282.28	-	-
75	-	315.19	1051	nd	$C_{20}H_{27}O_3^+$	1.42	269.19, 187.11	Unknown diterpene	Terpene
76	-	267.17	1078	nd	$C_{19}H_{23}O^+$	-3.17	211.11, 155.05	-	-

[a] denotes metabolites confirmed by matching to a standard.

list of the identified peaks with their UV and mass spectral data is shown in Table 2.

3.2. Flavonoids

Flavonoids were the most abundant secondary metabolite class observed with 19 identified peaks. The abundance of flavonoid conjugates can be seen in the total ion chromatogram within the elution region of t_R: 480–850 s (Fig. 3A and B). Late elution of the flavonoids is consistent with their nature as nonpolar metabolites compared to phenolic acids (Do et al., 2014).

Isorhamnetin was identified as the major flavonoid aglycone in most flavonoid conjugates with [M-H]$^-$ at *m/z* 315, after elimination of sugar residues; that is 162 amu for hexose sugar; glucose or galactose, 146 amu for deoxyhexose; rhamnose or 132 amu for pentoses (Otify, George, Elsayed, & Farag, 2015). For example, peak number 34 showed a molecular ion [M-H]$^-$ at *m/z* 785.21 with a molecular formula of; $(C_{34}H_{41}O_{21})^-$, yielding product ions at *m/z* 639 [M-146-H]$^-$, 477 [M-146-162-H]$^-$ and 315 [M-146-162-162-H]$^-$, a typical fragmentation pattern of isorhamnetin dihexosyl rhamnoside (Simirgiotis & Schmeda-Hirschmann, 2010). Another isorhamnetin conjugate was detected in peak 40 with a molecular ion [M-H]$^-$ at *m/z* 755.2 $(C_{33}H_{39}O_{20})^-$, and product ions at *m/z* 623 [M-132-H]$^-$ and 315 [M-132-146-162-H]$^-$ and identified as isorhamnetin pentosyl rutinoside (Ibrahim et al., 2015; Simirgiotis & Schmeda-Hirschmann, 2010). Similar fragmentation patterns were observed in flavonoid peaks 26, 28, 39, 42, 43, 44, 46, 49 and 56.

3.3. Phenolic and organic acids

Next to flavonoids, phenolic acids were the second most abundant secondary metabolites class detected in *O. ficus* represented by 11 peaks. Their abundance is visible within the total ion chromatogram at the elution region of t_R: 50–570 s (Fig. 3A and B), being most polar and eluting at high water eluent composition.

Peak number 5 showed a molecular ion [M-H]$^-$ at *m/z* 191.02 $(C_6H_7O_7)^-$ and gave a product ion at *m/z* 111 [M–CO_2–2H_2O–H]$^-$, a typical fragmentation pattern of (iso)citric acid (Yang et al., 2015). Among phenolic acids, peak number 7 showed a molecular ion [M-H]$^-$ at *m/z* 255.05 $(C_{11}H_{11}O_7)^-$ with product ions at *m/z* 237 [M–H_2O–H]$^-$, 193 [M–CO_2–2H_2O–H]$^-$, 165 [M–CO_2–CO–2H_2O–H]$^-$ and was identified as piscidic acid (Ginestra et al., 2009). Peaks 15, 19 and 21 showed similar fragmentation pattern with product ions at *m/z* 193 [M-R-H]$^-$ and 175 [M-R–H_2O–H]$^-$, ascribed to the loss of a ferulic acid moiety and suggesting that these metabolites are ferulic acid deriva-

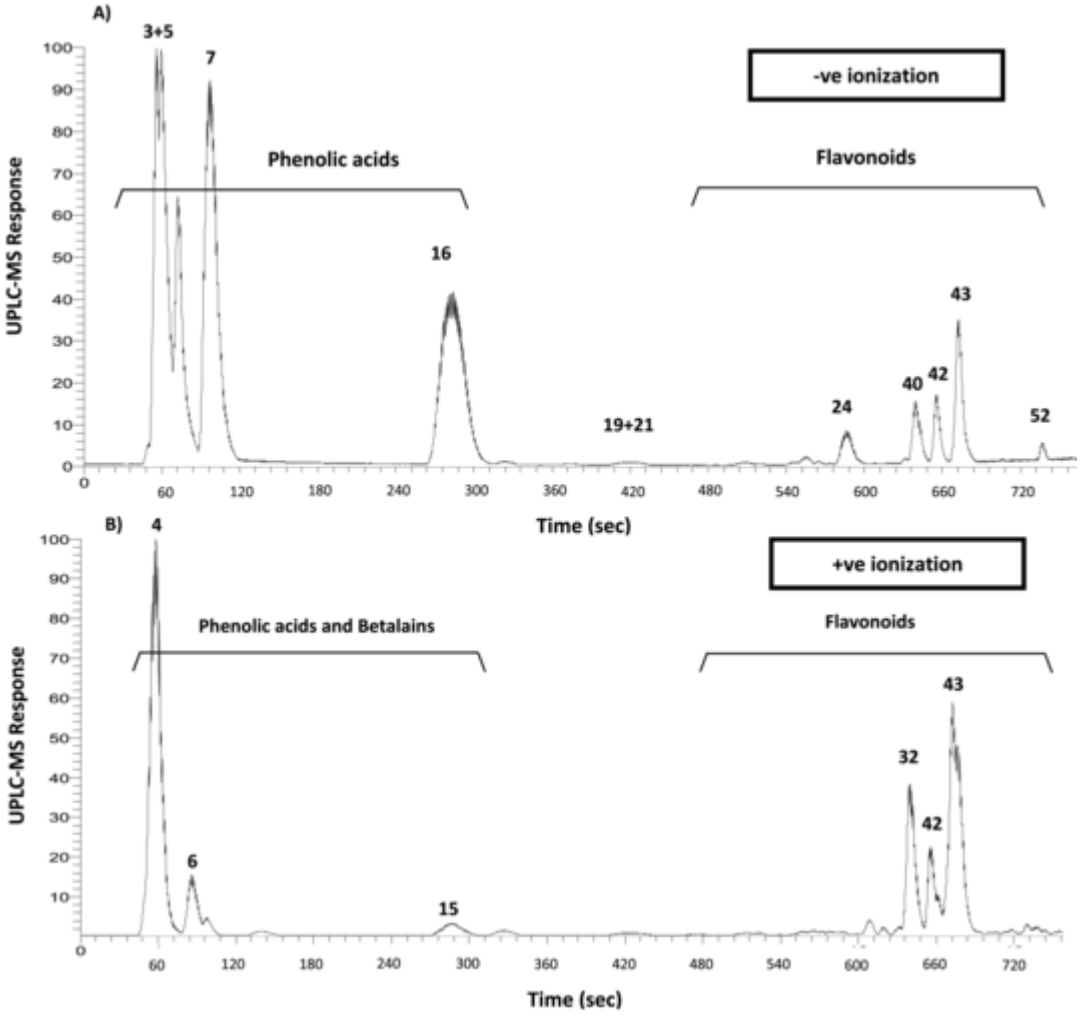

Fig. 3. - Representative UPLC-MS for *Opuntia ficus-indica* fruits Red 'Rose' cv A) negative ionization mode and B) positive ionization mode, both chromatograms are characterized using two regions; (50–570 s) for phenolic acids and (480–850 s) for flavonoids. Assigned peak numbers are shown in Table 2.

tives (Chahdoura et al., 2014). A sugar was identified in peak 3 with a molecular ion $[M\text{-}H]^-$ at *m/z* 195.05 $(C_6H_{11}O_7)^-$, and product ions at *m/z* 177 $[M–H_2O–H]^-$ and 159 $[M\text{-}2H_2O–H]^-$, a typical fragmentation pattern of gluconic acid (Deng & Yang, 2013). Gluconic acid was also detected in peak 21 identified as feruloyl gluconic acid from its spectral data (Table 2).

3.4. Betalains

The genus *Opuntia* is known to be rich in various metabolites belonging to the betalains class (Castellanos-Santiago & Yahia, 2008; Farag et al., 2017), however, only one metabolite belonging to the betaxanthin subclass was found. This might be due to the nature of the extraction procedure; pure alcoholic rather than hydroalcoholic extraction, which might not favour the polar nature of this metabolite class. Peak 6 showed a molecular ion $[M+H]^+$ at *m/z* 309.1 $(C_{14}H_{17}O_6N_2)^+$, with product ions at *m/z* 265 $[M + H–CO_2]^+$ and 219 $[M + H–2CO_2–2H]^+$, a typical fragmentation pattern of indicaxanthin (Msaddak et al., 2017).

3.5. Miscellaneous

Coumarins were among the minor classes of metabolites detected in fruit cvs found as dihydroxy psoralen-*O*-hexoside in peak 4. Peak 4 showed a molecular ion $[M+H]^+$ at *m/z* 381.07 $(C_{17}H_{17}O_{10})^+$, with product ions at *m/z* 219 $[M + H\text{-}162]^+$, 203 $[M + H\text{-}162\text{-}OH]^+$, 187 $[M + H\text{-}162\text{-}2OH]^+$ and 131 $[M + H\text{-}162\text{-}2OH–CO_2]^+$ (Wang et al., 2014). A few terpenes were also detected in fruit cvs among which was hydroxy-megastigmen-one-hexoside in peak 47. Peak 47 showed a molecular ion $[M\text{-}H]^-$ at *m/z* 371.2 $(C_{19}H_{31}O_7)^-$, with product ions at *m/z* 209.12 $[M\text{-}162\text{-}H]^-$, 181.05 $[M\text{-}162\text{-}CO\text{-}H]^-$, and 166.03 $[M\text{-}162\text{-}CO–CH_3–H]^-$. Chemical structures of major compounds identified in the text are shown in Fig. 4.

3.6. Multivariate data analysis of the UPLC-MS dataset

Multivariate data analysis of the UPLC-MS fruit metabolite profiles derived from the 3 cvs were used to assess the possible heterogeneity among cvs., The metabolites data were subjected to PCA and OPLS to discriminate between the different cvs and to determine which metabolite(s) has a greater impact in discriminating among the cvs. PC1 accounted for 48% of the cvs variance with the red cv peel (CRP1, CRP2, CRP3) positioned as the most distant with positive PC1 score values (Fig. 5). On the other hand, the green cv pulp (CGF1, CGF2, CGF3) were positioned to the far left (negative PC1 values). Green cv peel (CGP) and orange cv peel (COP) overlapped on the positive side along PC1. On the other hand, the red cv pulp (CRF) and orange cv pulp (COF) overlapped on the negative side of PC1. All cv pulp tissues had negative PC1 score values, while, the peels were clustered to the

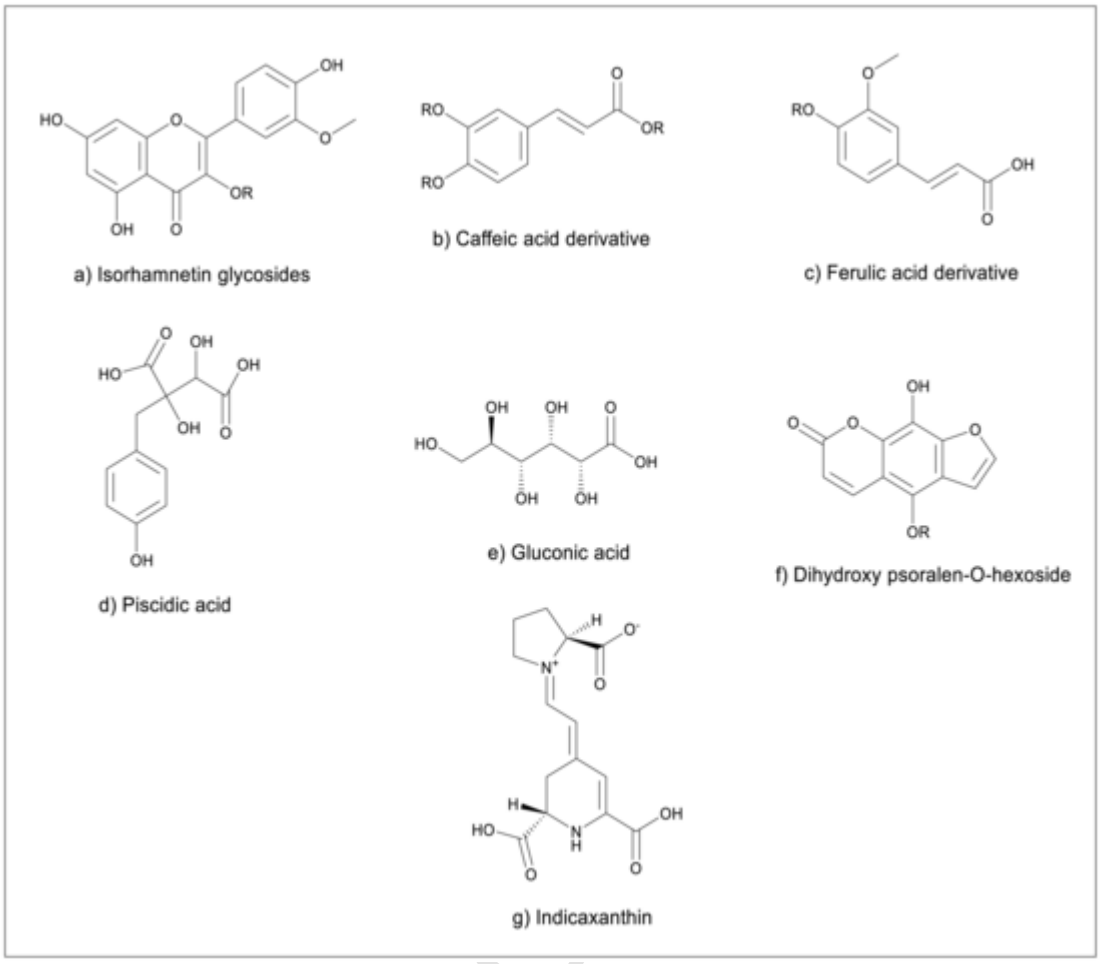

Fig. 4. - Chemical structures of detected metabolites in *O. ficus-indica* fruit cvs; a) isorhamnetin glycoside; R = dihexosyl rhamnose for peak number 34, R = pentosyl rutinose for peak number 40, b) caffeic acid derivative; peak number 37, c) ferulic acid derivative; peak numbers; 15, 19, 21, d) piscidic acid peak number 7, e) gluconic acid; peak number 3, f) dihydroxy psoralen-*O*-hexoside; R = hexose, peak number 4, g) indicaxanthin; peak number 6. All assigned peak numbers are shown in Table 2.

right (positive PC1 values) as shown in Fig. 5A, suggesting that fruit peel versus pulp overcomes the different cvcolors. Metabolites mediating for the discrimination were determined using the corresponding loading plot (Fig. 5B). Dihydroxy psoralen-*O*-hexoside was the most discriminating metabolite as evident from the loading plot suggesting that the red cv peel (CRP) had the highest coumarin levels. Additionally, the loading plot showed that ferulic acid and its glycosidic conjugates contributed to differences between peel and pulp among the different cvs (Fig. 5B).

Supervised multivariate data analyses using OPLS-DA is a good tool to assign markers characteristic for each fruit cv. In OPLS analysis, each fruit cv (pulp and peel) was assigned as one group and modelled versus all other cvs one at a time (Fig. 6A–C). Supervised multivariate statistical methods are required to estimate potential metabolite differences between samples from various species, especially when comparing several samples. OPLS allows comparing samples analyzed with different instruments and at different times. The OPLS model for the green cv modelled versus all cvs explained 81% of the total variance (R^2 = 0.81) with the prediction goodness parameter Q^2 = 0.60, while that of red and orange cv models (R^2 = 0.067, Q^2 = 0.42) and (R^2 = 0.71 and Q^2 = 0.20), respectively. The goodness of fit for the OPLS model described how well it fits a set of observations, and measures of goodness of fit typically summarize the discrepancy between observed values and the values expected with the OPLS model in question. The chemical distinctions shown from PCA were confirmed using OPLS-DA. The OPLS model for the greenish white cv versus the other cvs (Fig. 6A1 - 6A2) showed its increased indicaxanthin concurrent with lower coumarin levels exemplified by dihydroxy psoralen-*O*-hexoside. On the other hand, the OPLS model for the ''Rose'' cv (Fig. 6B1 - 6B2) showed that this cv has the highest amount of dihydrox psoralen-*O*-hexoside. With regards to the yellow-orange cv the OPLS scoring and loading S plots (Fig. 6C1 - 6C2) showed almost no chemical distinctions.

3.7. Antioxidant effect of O. ficus-indica cvs pulps and peels crude extracts

Free radicals have a significant role in the progression of oxidative stress (Seger & Sturm, 2007). The ability of methanol extracts prepared from cvs represented by pulp and peel specimens to scavenge free radicals *in-vitro* were assessed using DPPH and ABTS assays with ascorbic acid as the positive control. All cvs showed weaker antioxidant activities in both assays when compared to the ascorbic acid IC_{50} value of 4.1 mg ml^{-1} in ABTS assay. The red cv peel (CRP) which showed the highest antioxidant activity in both assays was found to be the most rich in dihydroxy psoralen-*O*-hexoside based on the PCA analysis and suggested that in ''Red'' ficus cv coumarins in addition to flavonoids increased the strong antioxidant activity. The green cv pulp (CGF), which showed the lowest antioxidant activity in both assays, showed the highest content of indicaxanthin (Fig. 7) suggesting that betalains are less active antioxidants compared to flavonoids and coumarins. These results were opposite to that of Albano et al. (2015), as they attributed the high antioxidant activity of the orange cv when

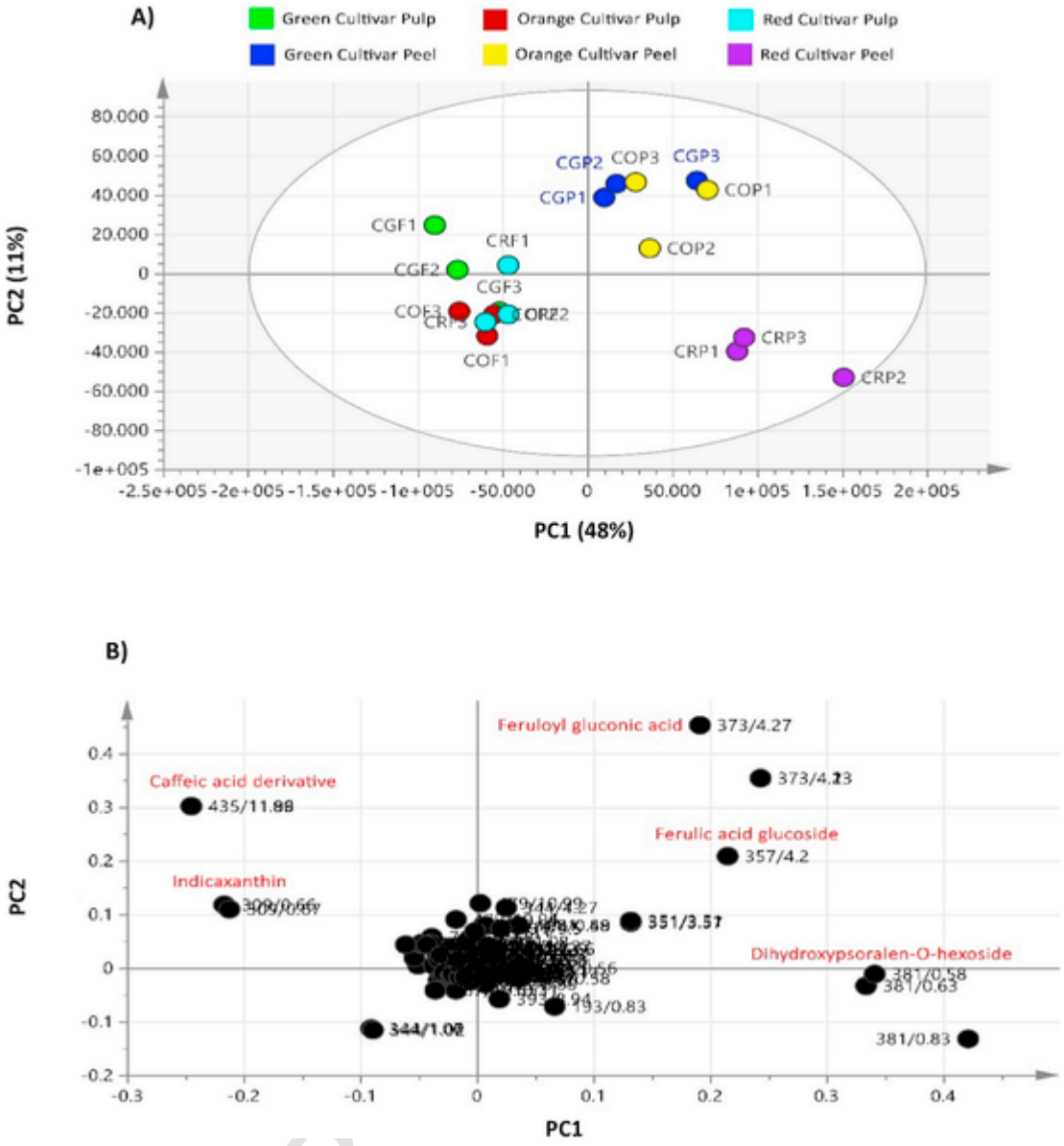

Fig. 5. - Principle component analysis of the metabolic analysis of all *O. ficus-indica* cvs shown in Table 2 clustered in two dimensional space at distinct positions and described by two vectors of principle component; PC1 = 48% and PC2 = 11%, a) shows a scoring plot describing PC1 versus PC2, while b) shows a loading plot for the contributing mass peaks and their assignments, each metabolite is denoted by its mass/retention time pair in min.

tested using ABTS assay to its high betaxanthin content despite having lower total phenolic content. Current results are consistent with that of Fernandez-Lopez, Almela, Obon, and Castellar (2010) where the antioxidant activity of the red cv of three *Opuntia* taxa which showed the highest total phenolic content, also had the lowest betalains content and had the highest antioxidant activity when tested using both ABTS and DPPH assays. On the other hand, Stintzing et al. (2005), showed that the antioxidant activity of different *Opuntia* species cvs using the ABTS assay was correlated with their high content of both total phenolics and betalains. Nevertheless, the likelihood of other polyphenolic compounds at low levels could act synergistically to affect the total antioxidant activities (Antunes-Ricardo, Gutiérrez-Uribe, Martínez-Vitela, & Serna-Saldívar, 2015). Antioxidant activity of most plant extract is attributed to the cumulative effect of many metabolites rather than a single compound.

4. Conclusions

A full metabolite profile of different cvs of *O. ficus-indica* using untargeted metabolite analyses was obtained. UPLC-UV-MS analysis coupled to multivariate data analyses showed that all cvs had no significant differences in their flavonoids level. However, the red cv was distinguished by its high coumarins levels. The presence of both flavonoids and coumarins are important for the strong antioxidant activity of the cv. Accordingly more attention should be paid to the red cv. Other compounds undetected using LC/MS might contribute to the observed antioxidant effects. To further determine the role of antioxidant phenolics in *O. ficus-indica* fruits, other antioxidant assays using different principles ought to be done such as; oxygen radical absorbance capacity, and total radical absorption potential. Additionally, isolated metabolites can be checked as well for their potential antioxidant activity. Metabolites identified herein as potential markers for each fruit cv may be posed as potential quality control markers for future standardization.

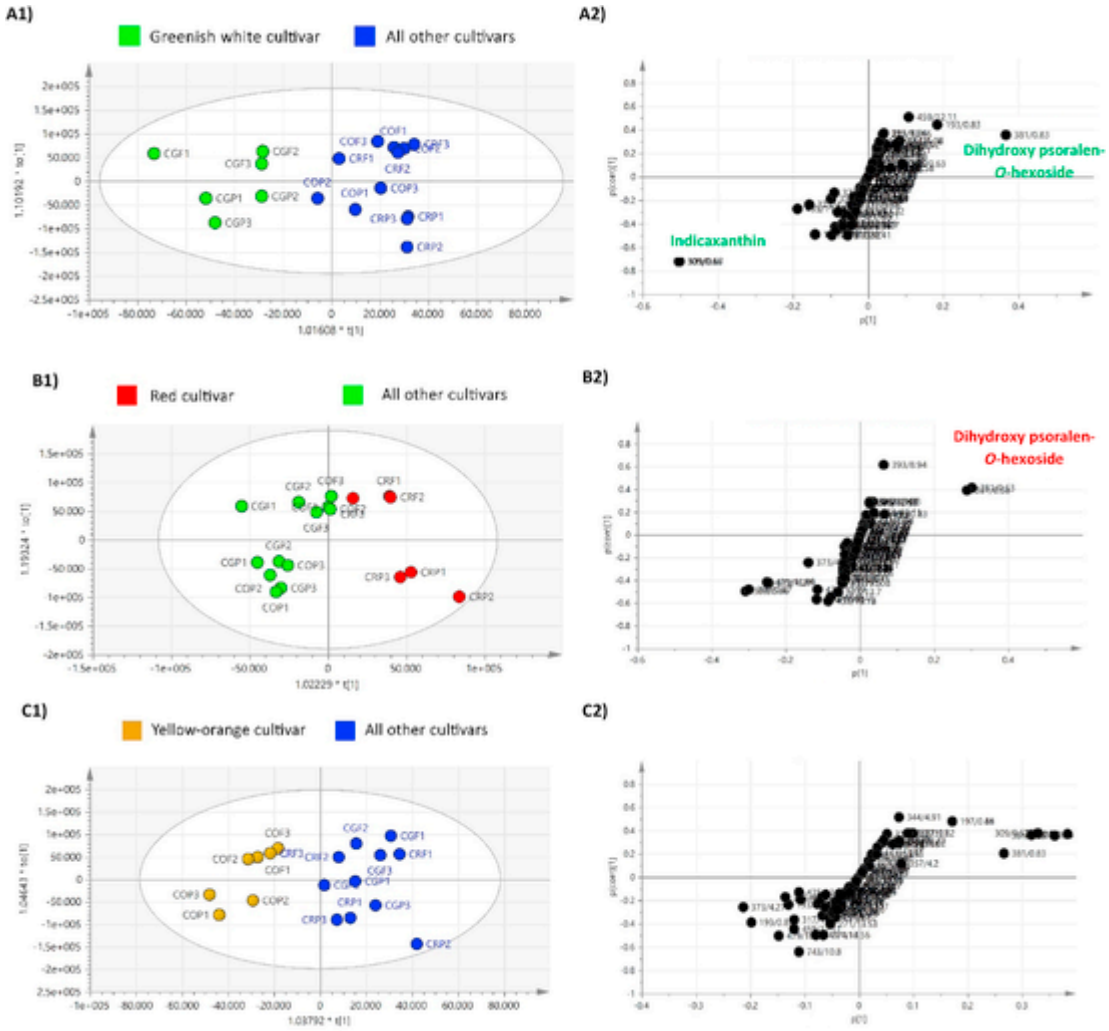

Fig. 6. - OPLS-DA plots for each cv versus other cvs; A1) score plot, A2) loading S plot of the greenish white cv vs. other cvs, B1) score plot, B2) loading S plot of the red cv vs. the other cvs, C1) score plot, C2) loading S plot of the yellow-orange cv vs other cvs, the selected variables for each plot are highlighted with their assignment and mass/retention time pair. (For interpretation of the references to color in this figure legend, the reader is referred to the Web version of this article.)

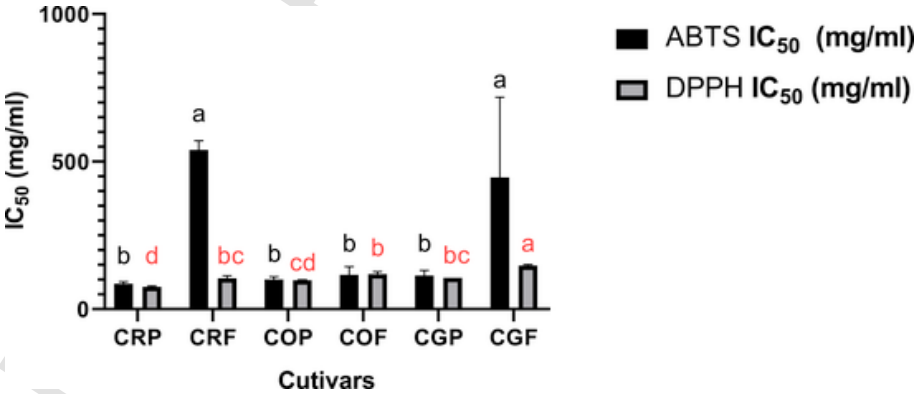

Fig. 7. - Antioxidant capacities of the three cvs of *O. ficus* measured using the ABTS and DPPH assays (n = 3). For samples abbreviations, refer to Table 1. Values are expressed as mean ± SEM. Statistical analysis was carried out using one-way ANOVA followed by Tukey's post hoc test. Unshared black letters between samples represent significance value at $p < 0.05$ in the ABTS assay, whereas unshared red letters between samples represent significance value at $p < 0.05$ in DPPH assay. (For interpretation of the references to color in this figure legend, the reader is referred to the Web version of this article.)

CRediT authorship contribution statement

Mohamed A. Farag: Conceptualization, Methodology, Resources. **Ibrahim E. Sallam:** Formal analysis, Writing - original draft. **Mostafa I. Fekry:** Validation, Software, Writing - review & editing. **Soumaya**

S. Zaghloul: Supervision. **Riham S. El-Dine:** Writing - review & editing.

Declaration of competing interest

The authors declare that there are no conflicts of interest with the work described in this manuscript.

Acknowledgements

Dr. Mohamed A. Farag acknowledges the funding received from Jesour grant number 30 from the Academy of Scientific Research and Technology (ASRT), Egypt and the Alexander von Humboldt Foundation, Germany. Special thanks to Anne Grate, Leibniz Institute of Plant Biochemistry, Halle Saale, Germany, for her kind assistance with the LC/MS measurements.

Appendix A. Supplementary data

Supplementary data to this article can be found online at https://doi.org/10.1016/j.fbio.2020.100673.

References

Albano, C, Negro, C, Tommasi, N, Gerardi, C, Mita, G, & Miceli, A, et al. (2015). Betalains, phenols and antioxidant capacity in cactus pear *[Opuntia ficus-indica (l.) mill.]* fruits from Apulia (south Italy) genotypes. Antioxidants (Basel), 4(2), 269–280. doi:10.3390/antiox4020269.

Ammar, I, Ennouri, M, Bouaziz, M, Ben Amira, A, & Attia, H (2015). Phenolic profiles, phytchemicals and mineral content of decoction and infusion of *Opuntia ficus-indica* flowers. Plant Foods for Human Nutrition (Dordrecht, Netherlands), 70(4), 388–394. doi:10.1007/s11130-015-0505-6.

Antunes-Ricardo, M, Gutiérrez-Uribe, J A, Martínez-Vitela, C, & Serna-Saldívar, S O (2015). Topical anti-inflammatory effects of isorhamnetin glycosides isolated from *Opuntia ficus-indica*. BioMed Research International, 1–9. doi:10.1155/2015/847320. 2015.

Castellanos-Santiago, E, & Yahia, E M (2008). Identification and quantification of betalains from the fruits of 10 Mexican prickly pear cultivars by high-performance liquid chromatography and electrospray ionization mass spectrometry. Journal of Agricultural and Food Chemistry, 56(14), 5758–5764. doi:10.1021/jf800362t.

Chahdoura, H, Barreira, J C M, Barros, L, Santos-Buelga, C, Ferreira, I C F R, & Achour, L (2014). Phytochemical characterization and antioxidant activity of *Opuntia microdasys (Lehm.)* Pfeiff flowers in different stages of maturity. Journal of Functional Foods, 9, 27–37. doi:10.1016/j.jff.2014.04.011.

De Leo, M, Abreu, M B De, Pawlowska, A M, Cioni, P L, & Braca, A (2010). Profiling the chemical content of *Opuntia ficus-indica* flowers by HPLC–PDA-ESI-MS and GC/EIMS analyses. Phytochemistry Letters, 3(1), 48–52. doi:10.1016/j.phytol.2009.11.004.

Deng, J, & Yang, Y (2013). Chemical fingerprint analysis for quality assessment and control of Bansha herbal tea using paper spray mass spectrometry. Analytica Chimica Acta, 785, 82–90. doi:10.1016/j.aca.2013.04.056.

Do, Q D, Angkawijaya, A E, Tran-Nguyen, P L, Huynh, L H, Soetaredjo, F E, & Ismadji, S, et al. (2014). Effect of extraction solvent on total phenol content, total flavonoid content, and antioxidant activity of *Limnophila aromatica*. Journal of Food and Drug Analysis, 22(3), 296–302. doi:10.1016/j.jfda.2013.11.001.

Farag, M A, Handoussa, H, Fekry, M I, & Wessjohann, L A (2016). Metabolite profiling in 18 Saudi date palm fruit cultivars and their antioxidant potential via UPLC-qTOF-MS and multivariate data analyses. Food and Function, 7(2), 1077–1086. doi:10.1039/c5fo01570g.

Farag, M A, Maamoun, A A, Ehrlich, A, Fahmy, S, & Wesjohann, L A (2017). Assessment of sensory metabolites distribution in 3 cactus *Opuntia ficus-indica* fruit cultivars using UV fingerprinting and GC/MS profiling techniques. Lebensmittel-Wissenschaft und -Technologie- Food Science and Technology, 80, 145–154. doi:10.1016/j.lwt.2017.02.014.

Fernandez-Lopez, J A, Almela, L, Obon, J M, & Castellar, R (2010). Determination of antioxidant constituents in cactus pear fruits. Plant Foods for Human Nutrition, 65(3), 253–259. doi:10.1007/s11130-010-0189-x.

Fernie, A R, Trethewey, R N, Krotzky, A J, & Willmitzer, L (2004). Metabolite profiling: From diagnostics to systems biology. Nature Reviews Molecular Cell Biology, 5(9), 763–769. doi:10.1038/nrm1451.

Ginestra, G, Parker, M L, Bennett, R N, Robertson, J, Mandalari, G, & Narbad, A, et al. (2009). Anatomical, chemical, and biochemical characterization of cladodes from prickly pear *[Opuntia ficus-indica (L.) Mill.]*. Journal of Agricultural and Food Chemistry, 57(21), 10323–10330. doi:10.1021/jf9022096.

Guevara-Figueroa, T, Jiménez-Islas, H, Reyes-Escogido, M L, Mortensen, A G, Laursen, B B, & Lin, L-W, et al. (2010). Proximate composition, phenolic acids, and flavonoids characterization of commercial and wild nopal (*Opuntia* spp.). Journal of Food Composition and Analysis, 23(6), 525–532. doi:10.1016/j.jfca.2009.12.003.

Ibrahim, R M, El-Halawany, A M, Saleh, D O, Naggar, E M B El, El-Shabrawy, A E-R O, & El-Hawary, S S (2015). HPLC-DAD-MS/MS profiling of phenolics from *Securigera securidaca* flowers and its anti-hyperglycemic and anti-hyperlipidemic activities. Revista Brasileira de Farmacognosia, 25(2), 134–141. doi:10.1016/j.bjp.2015.02.008.

Mata, A, Ferreira, J P, Semedo, C, Serra, T, Duarte, C M M, & Bronze, M R (2016). Contribution to the characterization of *Opuntia spp.* juices by LC-DAD-ESI-MS/MS. Food Chemistry, 210, 558–565. doi:10.1016/j.foodchem.2016.04.033.

Melgar, B, Pereira, E, Oliveira, M, Garcia-Castello, E M, Rodriguez-Lopez, A D, & Sokovic, M, et al. (2017). Extensive profiling of three varieties of *Opuntia spp.* fruit for innovative food ingredients. Food Research International, 101, 259–265. doi:10.1016/j.foodres.2017.09.024.

Msaddak, L, Abdelhedi, O, Kridene, A, Rateb, M, Belbahri, L, & Ammar, E, et al. (2017). *Opuntia ficus-indica* cladodes as a functional ingredient: Bioactive compounds profile and their effect on antioxidant quality of bread. Lipids in Health and Disease, 16(1), 32. doi:10.1186/s12944-016-0397-y.

Otify, A, George, C, Elsayed, A, & Farag, M A (2015). Mechanistic evidence of *Passiflora edulis* (Passifloraceae) anxiolytic activity in relation to its metabolite fingerprint as revealed via LC-MS and chemometrics. Food and Function, 6(12), 3807–3817. doi:10.1039/c5fo00875a.

Seger, C, & Sturm, S (2007). Analytical aspects of plant metabolite profiling platforms: Current standings and future aims. Journal of Proteome Research, 6(2), 480–497. doi:10.1021/pr0604716.

Simirgiotis, M J, & Schmeda-Hirschmann, G (2010). Direct identification of phenolic constituents in *Boldo Folium* (*Peumus boldus Mol.*) infusions by high-performance liquid chromatography with diode array detection and electrospray ionization tandem mass spectrometry. Journal of Chromatography A, 1217(4), 443–449. doi:10.1016/j.chroma.2009.11.014.

Stintzing, F C, Herbach, K M, Mosshammer, M R, Carle, R, Yi, W, & Sellappan, S, et al. (2005). Color, betalain pattern, and antioxidant properties of cactus pear (*Opuntia spp.*) clones. Journal of Agricultural and Food Chemistry, 53(2), 442–451. doi:10.1021/jf048751y.

Wang, F, Liu, N, Xiong, W, Yan, M, Zhu, Y, & Gao, M, et al. (2014). A UPLC-MS/MS method for *in vivo and in vitro* pharmacokinetic studies of psoralenoside, isopsoralenoside, psoralen and isopsoralen from *Psoralea corylifolia* extract. Journal of Ethnopharmacology, 151(1), 609–617. doi:10.1016/j.jep.2013.11.013.

Wolfender, J L, Marti, G, Thomas, A, & Bertrand, S (2015). Current approaches and challenges for the metabolite profiling of complex natural extracts. Journal of Chromatography A, 1382, 136–164. doi:10.1016/j.chroma.2014.10.091.

Yang, L, Lu, M, Carl, S, Mayer, J A, Cushman, J C, & Tian, E, et al. (2015). Biomass characterization of Agave and *Opuntia* as potential biofuel feedstocks. Biomass and Bioenergy, 76, 43–53. doi:10.1016/j.biombioe.2015.03.004.